CHALMERS
UNIVERSITY OF TECHNOLOGY

Comparison of Additively Manufactured and Machined Antenna Array Performance at Ka-Band

Downloaded from: https://research.chalmers.se, 2026-10-15 18:00 UTC

Citation for the original published paper (version of record):
Kahkonen, H., Proper, S., Ala-Laurinaho, J. et al (2022). Comparison of Additively Manufactured and Machined Antenna Array Performance at Ka-Band. IEEE Antennas and Wireless Propagation Letters, 21(1): 9-13. http://dx.doi.org/10.1109/LAWP.2021.3113372

N.B. When citing this work, cite the original published paper.

© 2022 IEEE. Personal use of this material is permitted. Permission from IEEE must be obtained for all other uses, in any current or future media, including reprinting/republishing this material for advertising or promotional purposes, or reuse of any copyrighted component of this work in other works.

(article starts on next page)

Comparison of Additively Manufactured and Machined Antenna Array Performance at *Ka*-Band

Henri Kähkönen, Sebastian Proper, Juha Ala-Laurinaho, and Ville Viikari, *Senior Member, IEEE*

***Abstract*—Additive manufacturing (AM) is a rapidly developing field, which potentially decreases the manufacturing costs and enables increasingly complex antenna shapes. Metal-based AM might be particularly useful for manufacturing antennas at millimeter-wave (mm-wave) range, because these antennas are physically small enough making AM cost efficient, and manufacturing accuracy could still suffice for good electrical performance. In this letter, two additively manufactured and identical machined fully metallic Ka-band Vivaldi antenna arrays are compared. The manufactured antenna arrays are compared using RF measurements to conclude the feasibility of AM for manufacturing antenna arrays at mm-wave frequencies. Comparison of the measured radiation patterns and realized gains of each of the antenna arrays between 26 and 40 GHz shows close to identical radiation patterns for all the arrays. A loss in realized gain of 0.5–1.5 dB is observed in the AM arrays when compared to the machined array due to the used materials and the surface roughness.**

***Index Terms*—Additive manufacturing (AM), antenna array, flared-notch antenna, millimeter wave (mm-wave), phased array, tapered slot, Vivaldi antenna, fifth-generation (5G).**

I. Introduction

VIVALDI antenna elements are very attractive for antenna arrays due to their performance. Vivaldi arrays can be made dual polarized without increasing the element footprint, they can be made wideband while maintaining small interelement distance, and they can provide relatively high efficiency and large beam steering range as compared to arrays realized solely on a printed circuit board (PCB) [1], [2]. These antenna arrays can be manufactured with a few different manufacturing methods, for example, manufacturing the antenna array from a single piece of metal using wire electric discharge machining (WEDM) and manufacturing the array from multiple separate parts using conventional machining methods or on a PCB arranged in a grid pattern. These manufacturing methods have been widely used for frequencies below 20 GHz [1]–[4]. While arrays even up to 40 GHz have been manufactured using WEDM [5], the manufacturing of such antenna arrays becomes increasingly more demanding and expensive for higher frequencies and requires advanced skills in wire cutting and machining.

The emergence of additive manufacturing (AM) has increased the available methods for fabrication of complex shapes. Promising methods for producing metallic antenna arrays are metallizing additively manufactured plastic parts and direct metal printing, such as selective laser melting (SLM) or binder jetting [6]–[11]. Direct metal printing methods are based on fusing small-metal powder particles together, either by melting or by sintering, directly forming the final structure.

Even though AM at first glance looks like the perfect solution for manufacturing complex antenna shapes, there are still a number of open questions. One of the problems in metal printing is the surface roughness of the printed parts for applications operating at or above millimeter-wave (mm-wave) frequencies [8]. As printing is based on melting or sintering small metal particles, these will create a microscale pattern on the surface of the part, and the pattern depends on the particle size and other parameters related to the printing technology. Additionally, partially or completely melting materials can cause random variation in the final dimensions of the structure. On the other hand, small metal-plated plastic part can suffer from lower structural rigidity, and they cannot be used as heat sinks for cooling active electronics.

In this letter, we extend the research on the Vivaldi antenna array design presented in [5] and [12] by demonstrating the use of AM processes, namely, SLM and binder jetting to manufacture the fully metallic antenna array. While AM has been demonstrated in horn antenna elements even above 200 GHz [11], it has yet to be demonstrated on more complex antenna array geometries at mm-wave frequencies. This letter shows AM applied on a mechanically complex antenna array structure with small gaps and features, such as the coaxial feed pin and the narrow gap that is fed by the coaxial line, which are challenging and expensive to manufacture using conventional machining. This letter concentrates on comparing the achieved performance between conventionally and AM fully metallic antenna arrays at mm-wave frequencies.

II. Antenna Array

This comparison uses rectangular 8×8 Ka-band antenna arrays with 64 dual-polarized antenna elements. A single dual-polarized antenna element occupies a volume of

Manuscript received August 16, 2021; accepted September 12, 2021. Date of publication September 20, 2021; date of current version January 12, 2022. This work was supported in part by Saab Ab and in part by Vinnova (Swedish Energy Agency) and FORMAS through the Project AMLIGHT within the Strategic Innovation Programme Metallic Materials under Grant 2018-00798. *(Corresponding author: Henri Kähkönen.)*

Henri Kähkönen is with the Department of Electronics and Nanoengineering, Aalto University, 00076 Espoo, Finland, and also with Saab Finland Oy, 00100 Helsinki, Finland (e-mail: henri.kahkonen@aalto.fi).

Sebastian Proper is with the Department of Industrial and Materials Science, Chalmers University, 412 96 Gothenburg, Sweden, and also with RISE AB, 501 15 Borås, Sweden (e-mail: sebastian.proper@ri.se).

Juha Ala-Laurinaho and Ville Viikari are with the Department of Electronics and Nanoengineering, Aalto University, 00076 Espoo, Finland (e-mail: juha.ala-laurinaho@aalto.fi; ville.viikari@aalto.fi).

Digital Object Identifier 10.1109/LAWP.2021.3113372

This work is licensed under a Creative Commons Attribution 4.0 License. For more information, see https://creativecommons.org/licenses/by/4.0/

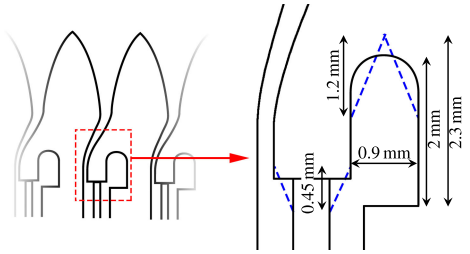

Fig. 1. Cross-sectional illustration of the differences between the geometry in the antenna feed and the cavity in case of the machined and the AM antennas. The solid line illustrates the profile of the machined antenna element and the dashed lines illustrate the modifications required for AM.

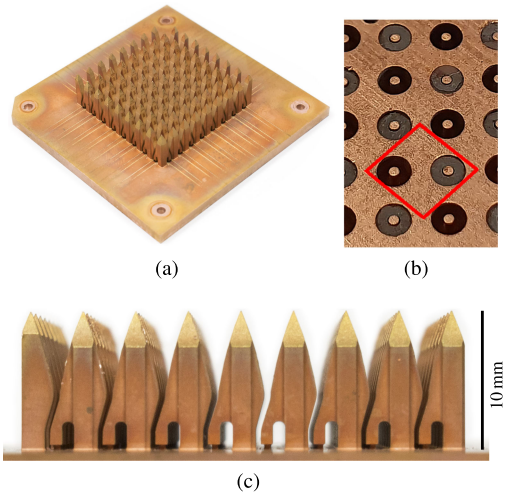

Fig. 2. Machined copper array. (a) Whole structure. (b) Part of the coaxial antenna feeds on the bottom of the array including a square illustrating one antenna unit. (c) Side profile of the antenna elements.

$3.8 \times 3.8 \times 10$ mm^3 ($x \times y \times z$). According to unit-cell simulations, the antenna element design has a beam steering range of $\pm 60^\circ$ between 26 and 40 GHz [5]. In the initial design of the antenna element, some of the requirements for manufacturing the antenna with AM have already been taken into account, such as the minimization of downward-facing planes and consideration for the smallest possible printable geometries. However, additional modifications were necessary to facilitate the requirements in the SLM process. The most significant modifications are the tapered roof of the cavity and a constant taper from the coaxial feeding pin to the point where the pin attaches to the antenna structure, as shown in the cross-sectional illustration of the antenna elements in Fig. 1. The modifications have been designed such that they have a negligible effect on the performance of the antenna.

The reference array in Fig. 2 is used as a comparison to the AM antenna arrays. It is machined from a solid block of copper using WEDM and conventional milling. The active area of the array is 30.4×30.4 mm^2, and the ground plane around the antenna elements extends 14.8 mm in each direction. The total size of the structure including the extended ground plane is $60 \times 60 \times 13$ mm^3.

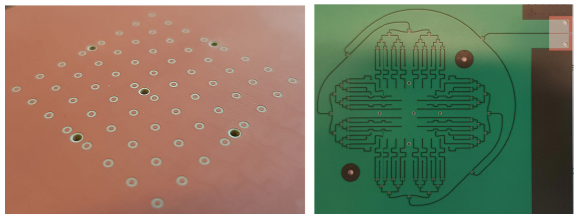

Fig. 3. (a) Antenna feeding pads on the PCB for one polarization. (b) Feeding network on the other side of the PCB.

Two AM antenna arrays were manufactured using two different manufacturing methods, one with SLM and the other with binder jetting. The material used in the SLM is aluminum alloy (AlSi10Mg) with a bulk electrical conductivity of approximately 2×10^7 S/m, while stainless steel (316 L) with a bulk electrical conductivity of approximately 1.3×10^6 S/m is used in binder jetting.

Due to the very small size of the antenna elements and consequently the high density of the antenna feeds, it is extremely difficult to use separate RF connectors and cables for each antenna element. Instead of feeding each antenna element directly with a cable, the antenna array is surface mountable, and the elements are fed with air-filled coaxial transmission lines, which are integrated in the structure and pass through the antenna ground plane [12]. The coaxial transmission lines in the antenna structure couple capacitively to circular pads on the PCB shown in Fig. 3(a). The pads are connected to a feed network consisting of a tree of 1-to-2 power dividers such that they form a 1-to-64 power division for one polarization, which is shown in Fig. 3(b). In this demonstration, where the manufacturing methods are compared, a fixed feed network for one polarization is used for smaller amount of uncertainties. A more thorough analysis of the feed network with beam steering is presented in [12].

A. *Selective Laser Melting*

SLM is a powder bed process, in which the metal powder is melted together with a laser and, layer by layer, the part is formed. Each layer is melted with an optimum energy density that melts some of the previously melted layers, resulting in manufactured parts that are recognized by their high strength and low porosity [13], [14]. On the other hand, high surface roughness and limited dimensional control of small features are drawbacks with the technique [15]. In the SLM process, the aluminum alloy AlSi10Mg is used due to its commercial availability, relatively fast production, and good surface finish compared to other materials available for the SLM process.

The manufactured antenna array in Fig. 4 shows the limitations with the process. The shape is less consistent in this model as compared to the arrays manufactured with machining and binder jetting. On the surfaces, the melting of the powder particles has caused some balling, which can be seen especially on the upper part of the array. Additionally, noticeable "edge effect" can be seen around the elements, which is caused by the laser movement, e.g., start and stop, resulting in more melted

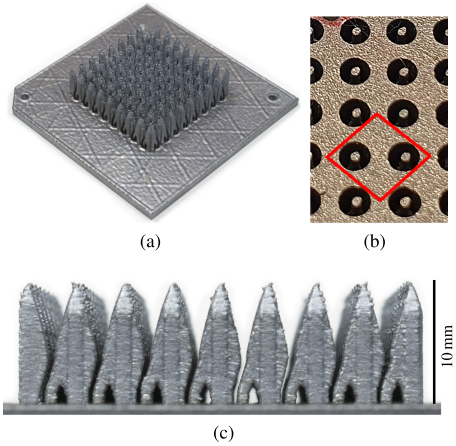

Fig. 4. Antenna array that is manufactured with the SLM process using aluminum alloy powder. (a) Whole structure. (b) Part of the coaxial antenna feeds on the bottom of the array including a square illustrating one antenna unit. (c) Side profile of the antenna elements.

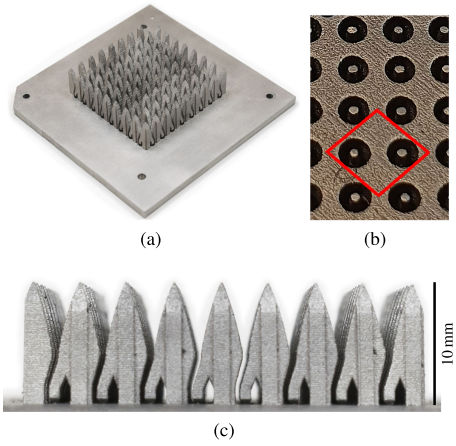

Fig. 5. Antenna array that is manufactured with the binder jetting process using steel powder. (a) Whole structure. (b) Part of the coaxial antenna feeds on the bottom of the array including a square illustrating one antenna unit. (c) Side profile of the antenna elements.

material in corners. On the other hand, the layers are not as prominent as in the binder jetting antenna array due to the remelting of previous layer reducing the distinct line between the layers.

B. Binder Jetting

Binder jetting with metal powder is a multistep process, which is also based on the powder bed process but uses a different method for fusing the material than SLM [16], [17]. In the first step, the metal powder is bound together using a liquid binding agent layer by layer. After the structure is printed, it is placed in a high-temperature oven, where the binding agent is decomposed and the metal particles are sintered together to form the final part. Depending on the density of the material before sintering, the final part usually shrinks by 15%–20%. This method of manufacturing usually results in slightly better dimensional accuracy than SLM due to the powder not melting completely during the sintering, assuming that the shrinkage during the process is well known.

The array manufactured with binder jetting uses the same 3-D model as the SLM print. Stainless steel powder was selected as the material as aluminum was not available with the process at the time of manufacturing. Fig. 5 shows the manufactured antenna array. The shape of the resulting antenna array is very close to the model, and all the details are well defined. The structure has been formed precisely, although its surface seems a rough due to the powder particles. Compared to the SLM array, the overall shape of this antenna array is closer to the model with less surface imperfection.

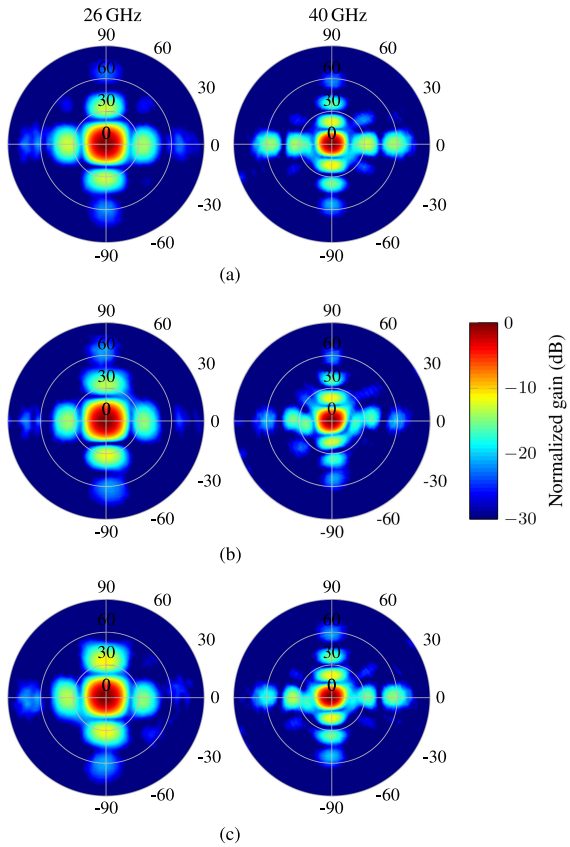

Fig. 6. Comparison of the measured normalized far-field pattern of each antenna array at 26 and 40 GHz. (a) Machined array. (b) SLM array. (c) Binder jetting array.

III. Measurement Results

Far-field measurements are used to evaluate the performance of the AM antennas in comparison to the machined array. All the arrays are measured in an anechoic chamber with an excitation resulting in a broadside beam.

Fig. 6 shows the measured normalized far-field patterns at 26 and 40 GHz. The shape of the patterns is very similar at 26 GHz in all the measured antennas. At 40 GHz, the radiation patterns of the AM arrays are still close to the reference pattern, but there are some discrepancies in the sidelobe levels in the E-plane ($\phi = 0°$).

Further comparison of the radiation patterns is shown in Fig. 7, where normalized radiation patterns in E- and H-planes are

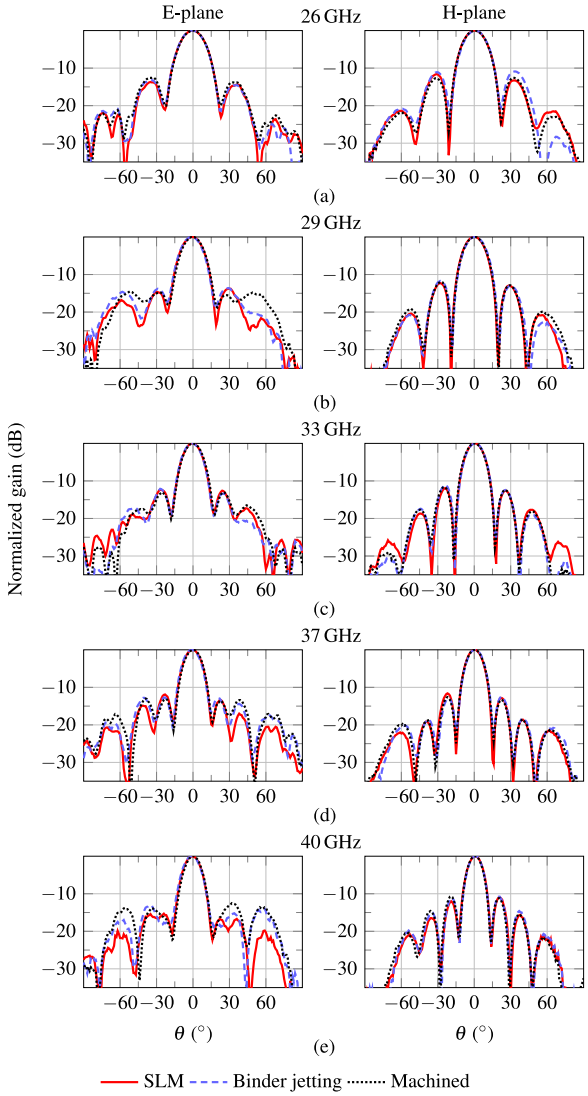

Fig. 7. Measured radiation patterns of the three antenna arrays at (a) 26, (b) 29, (c) 33, (d) 37, and (e) 40 GHz in E- and H-planes.

presented at 26, 29, 33, 37, and 40 GHz. The E-plane pattern is shown in the first column and the H-plane pattern in the second one. The match between the arrays is good throughout the specified frequency band. Only the smaller sidelobes are slightly affected in the E-plane; however, the overall sidelobe levels are similar for all the manufactured antennas.

The realized gain of the antennas is used to compare the losses in the AM antenna structures due to the surface roughness and limited material conductivity to the losses in the machined array. Fig. 8 shows the measured realized gains and the gain difference between the AM arrays and the machined array. There is 0.5–1.5 dB additional loss in the AM arrays when compared to the machined array. However, the gain-difference variation for the SLM array shows three distinct spikes at 30, 36.5, and 39 GHz. This difference might be caused by the higher inconsistency in the surface of the SLM array or some other imperfection

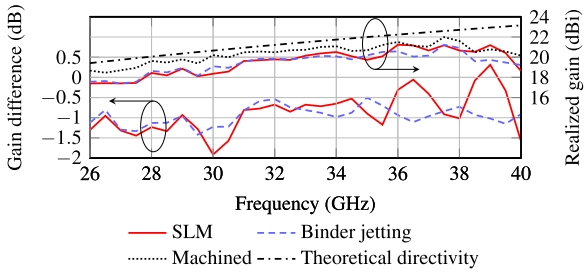

Fig. 8. Measured realized gains of the antenna arrays and the gain difference of the two AM arrays when compared to the machined array.

in the printed structure causing unwanted reflections in the antenna.

Finally, simulations are used to find realistic values for the surface roughness that correspond to the loss in efficiency in the measurement results. The simulations show that surface roughness values of 15 and 12 μm are found to correspond well with the measurements of the SLM and binder jetting antennas, respectively. In both cases, the loss in realized gain and effectively the total efficiency, when compared to a simulation where the copper array is used, is on average 1 dB.

IV. Conclusion

This letter presented a comparison between a machined copper antenna array and two AM arrays, one printed in aluminum alloy using SLM and the other printed in stainless steel using binder jetting. The antenna arrays are surface-mounted dual-polarized 8×8 Vivaldi antenna arrays. Measurements are performed by feeding one polarization of the array. The measured radiation patterns of the AM antenna arrays match well with the machined antenna array despite the higher surface roughness and a number of surface imperfections, in particular, in the case of the SLM.

The gain measurement is used to compare the losses of the antenna arrays due to the surface roughness and other manufacturing imperfections. The measurements show a decrease of 0.5–1.5 dB in the realized gain of the AM arrays. Additionally, results in the case of SLM suggest imperfections in the printed part causing reflections in the structure.

The presented results prove that it is possible to use AM, such as SLM or binder jetting, to build antenna arrays even up to 40 GHz without major impact on the antenna performance. Even though some of the geometries in the presented array are at the edge of the current AM capabilities, the results show good agreement between the AM and conventionally machined antenna array measurements. Additionally, the use of AM simplifies the manufacturing process of parts that can be challenging to manufacture with conventional methods.

Acknowledgment

The authors would like to thank the project steering group at Saab for discussions and feedback during the project and the participants of the AMLIGHT project.

REFERENCES

[1] H. Holter, "Dual-polarized broadband array antenna with BOR-elements, mechanical design and measurements," *IEEE Trans. Antennas Propag.*, vol. 55, no. 2, pp. 305–312, Feb. 2007.

[2] R. W. Kindt and W. R. Pickles, "Ultrawideband all-metal flared-notch array radiator," *IEEE Trans. Antennas Propag.*, vol. 58, no. 11, pp. 3568–3575, Nov. 2010.

[3] H. Holter, T.-H. Chio, and D. H. Schaubert, "Experimental results of 144-element dual-polarized endfire tapered-slot phased arrays," *IEEE Trans. Antennas Propag.*, vol. 48, no. 11, pp. 1707–1718, Nov. 2000.

[4] R. Kindt and J. Logan, "Benchmarking ultrawideband phased antenna arrays: Striving for clearer and more informative reporting practices," *IEEE Antennas Propag. Mag.*, vol. 60, no. 3, pp. 34–47, Jun. 2018.

[5] H. Kähkönen, J. Ala-Laurinaho, and V. Viikari, "Dual-polarized Ka-band Vivaldi antenna array," *IEEE Trans. Antennas Propag.*, vol. 68, no. 4, pp. 2675–2683, Apr. 2020.

[6] J. Massman, G. Simpson, and T. Steffen, "Low cost additively manufactured antenna array modules," in *Proc. IEEE Int. Symp. Phased Array Syst. Technol.*, 2019, pp. 1–4.

[7] S. Gill, H. Arora, Jidesh, and V. Sheth, "On the development of antenna feed array for space applications by additive manufacturing technique," *Additive Manuf.*, vol. 17, pp. 39–46, 2017.

[8] E. García-Marín, J. L. Masa-Campos, P. Sánchez-Olivares, and J. A. Ruiz-Cruz, "Evaluation of additive manufacturing techniques applied to Ku-band multilayer corporate waveguide antennas," *IEEE Antennas Wireless Propag. Lett.*, vol. 17, no. 11, pp. 2114–2118, Nov. 2018.

[9] G. Cung, T. Spence, and P. Borodulin, "Enabling broadband, highly integrated phased array radiating elements through additive manufacturing," in *Proc. IEEE Int. Symp. Phased Array Syst. Technol.*, 2016, pp. 1–9.

[10] G. Huang, S. Zhou, and T. Yuan, "Development of a wideband and high-efficiency waveguide-based compact antenna radiator with binder-jetting technique," *IEEE Trans. Compon., Packag., Manuf. Technol.*, vol. 7, no. 2, pp. 254–260, Feb. 2017.

[11] B. Zhang *et al.*, "Metallic 3-D printed antennas for millimeter- and submillimeter wave applications," *IEEE Trans. THz Sci. Technol.*, vol. 6, no. 4, pp. 592–600, Jul. 2016.

[12] H. Kähkönen, J. Ala-Laurinaho, and V. Viikari, "Surface-mounted Ka-band Vivaldi antenna array," *IEEE Open J. Antennas Propag.*, vol. 2, pp. 126–137, 2021.

[13] A. Leicht, U. Klement, and E. Hryha, "Effect of build geometry on the microstructural development of 316 L parts produced by additive manufacturing," *Mater. Characterization*, vol. 143, pp. 137–143, 2018.

[14] N. Read, W. Wang, K. Essa, and M. M. Attallah, "Selective laser melting of AlSi10Mg alloy: Process optimisation and mechanical properties development," *Mater. Des.*, vol. 65, pp. 417–424, 2015.

[15] X. Han, H. Zhu, X. Nie, G. Wang, and X. Zeng, "Investigation on selective laser melting AlSi10Mg cellular lattice strut: Molten pool morphology, surface roughness and dimensional accuracy," *Materials*, vol. 11, no. 3, 2018, Art. no. 392.

[16] M. Ziaee and N. B. Crane, "Binder jetting: A review of process, materials, and methods," *Additive Manuf.*, vol. 28, pp. 781–801, 2019.

[17] M. Li, W. Du, A. Elwany, Z. Pei, and C. Ma, "Metal binder jetting additive manufacturing: A literature review," *J. Manuf. Sci. Eng.*, vol. 142, no. 9, 2020, Art. no. 090801.